

Simulating Typhoon Floods with Gauge Data and Mesoscale-Modeled Rainfall in a Mountainous Watershed

MING-HSU LI, MING-JEN YANG, AND RUITANG SOONG

Institute of Hydrological Sciences, National Central University, Jung-Li, Taiwan

HSIAO-LING HUANG

Institute of Geography, Chinese Culture University, Taipei, Taiwan

(Manuscript received 8 June 2004, in final form 26 November 2004)

ABSTRACT

A physically based distributed hydrological model was applied to simulate typhoon floods over a mountainous watershed in Taiwan. The meteorological forcings include the observed gauge rainfall data and the predicted rainfall data from a mesoscale meteorological model, the fifth-generation Pennsylvania State University–National Center for Atmospheric Research (PSU–NCAR) Mesoscale Model (MM5). This study investigates the flood responses of three Typhoons: Zeb (1998), Nari (2001), and Herb (1996), which possessed unique meteorological features and that all produced severe floods. The predicted basin-averaged rainfall hydrographs by the MM5 are compared with that interpreted by rain gauge data to reveal the discrepancies in rainfall peak amounts and time lags, and to explore their subsequent effects on flood generation. The simulated flood hydrographs at the Hsia-Yun station, which is upstream of the Shihmen Reservoir, are compared with observed flood discharges in terms of the amount and time lag of flood peaks. It is shown that the small discrepancy in rainfall peaks and phase lags could be significantly amplified in simulated flood responses of a mountainous watershed. The overall predictive skill of the distributed hydrological model with different rainfall inputs is examined with three parameters, which include the runoff ratio (RR), root-mean-square error (rmse), and goodness of fit (GOF). Although the runoff ratio for the MM5-predicted rainfall is superior to that for the observed gauge rainfall, the simulated hydrographs with observed gauge rainfall have smaller rmse and GOF values for three events. This study shows that the error in flood prediction with the mesoscale-modeled rainfall is mainly caused by the rainfall–peak difference, which arises from the inherent uncertainties in the mesoscale-modeled rainfalls over a mountainous terrain during the typhoon landfall periods.

1. Introduction

Typhoons are recognized as one of the most devastating natural hazards in Taiwan. Between 1949 and 2003, an annual average of 3.6 typhoons (261 typhoons totally) invaded this subtropical complex-terrain island and its vicinity (Fig. 1). Subsequent flooding and associated gusty winds resulted in severe casualties and an average annual loss of more than 500 million U.S. dollars in agricultural, economical, and infrastructure damages. In addition to structural mitigation measures, such as levees or flood-control reservoirs, a better flood forecasting capability and timely flood warnings are highly needed, and this requires a multidiscipline cooperation between hydrologists and meteorologists.

Corresponding author address: Ming-Hsu Li, Assistant Professor, Institute of Hydrological Sciences, National Central University, Jung-Li, 320, Taiwan.
E-mail: mli@cc.ncu.edu.tw

River basins in Taiwan are typically very steep and narrow at the upstream end over the Central Mountain Range, with a meandering river over a mild terrain slope at midstream, and then have a widespread alluvial plain at the downstream end. The most significant hydrological manifestations of such river geomorphologic features are a short flood concentration time and a high peak as a result of fast basin flood responses. During typhoon landfall periods (the typhoon season is mainly July to October in Taiwan), the amount and timing of reservoir storage discharges need to be advised in advance with the predicted inflow to avoid aggravating the downstream flood, endangering dam safety, and wasting valuable water resources. Accurate prediction of typhoon floods is thus very important to reservoir operation and flood mitigation in Taiwan.

Simulating typhoon flood responses over the mountainous watersheds in the Taiwan area presents a unique challenge for hydrometeorological research. In the meteorological aspect, the interactions between ty-

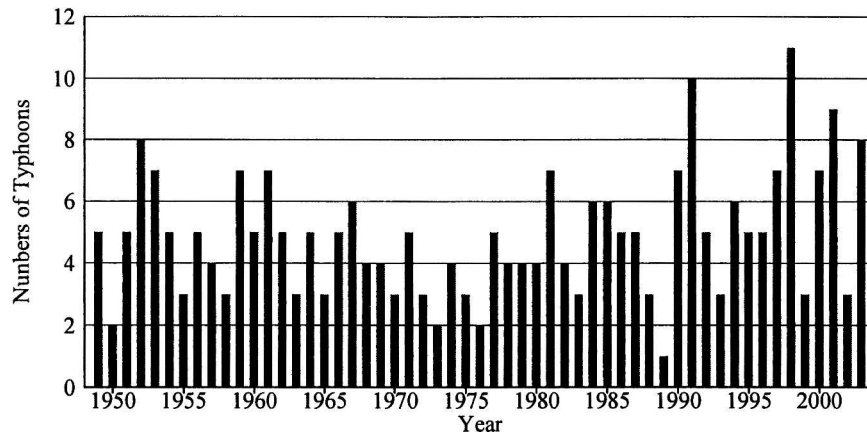


FIG. 1. Number of typhoons invading Taiwan and its vicinity from 1949 to 2003.

phoon vortex circulation and Taiwan’s mountainous terrain (mainly the north–south-orientated Central Mountain Range; see Fig. 2) increase uncertainties and difficulties in the typhoon track and the resulting rainfall predictions (Chang 1982; Wu and Kuo 1999). A mesoscale meteorological model with nonhydrostatic dynamics, high spatial resolution, and adequate precipitation parameterization is required to resolve a typhoon’s convective-scale structure and its associated rainfall. In the hydrological part, flooding responses to the typhoon rainfall involve complex interactions between the terrain effects and the relevant land hydrological processes, such as surface runoffs, channel flows,

interceptions, infiltration, and groundwater baseflows. Owing to the steep surface slopes in the upstream watersheds over Taiwan, typhoon flood hydrographs normally have large peaks with fast-rising limbs. Although physically based distributed hydrological models are suitable for characterizing these complicated interactions and heterogeneity in mountainous watersheds, improper spatial and temporal resolutions and inadequate interpretation of the land hydrological processes may significantly affect the modeling skill (Thielen et al. 1999; Smith et al. 2002; Wigmosta et al. 1994; Dutta et al. 2000; Morrison and Smith 2001).

Accurate rainfall information is crucial in modeling

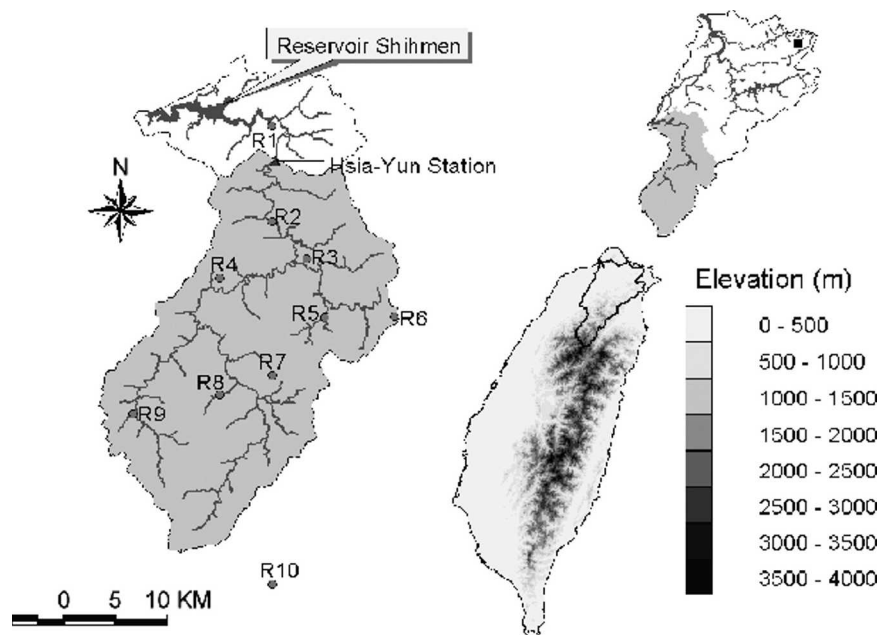


FIG. 2. (left) Hsia-Yun watershed of (upper right) Tamsui River basin in Taiwan [(bottom right) the north–south-orientated Central Mountain Range]. R1 to R10 indicates the locations of gauge stations, and the square symbol in the upper right is the location of the Wu-Fen Mountain radar station.

basin flood responses because it is the most important forcing for a hydrologic model during typhoon events (Zhang and Smith 2003). Spatial variability of rainfall can translate into significant variations of simulated runoff peaks and phases (Faures et al. 1995; Syed et al. 2003). For flood warnings, ground-based gauge stations are incapable of providing information with sufficient leadtime because of quick flood concentration time in Taiwan. Although the Doppler surveillance radar can provide estimates of the spatial rainfall distribution for flood predictions (Giannoni et al. 2003), the availability and accuracy of these rainfall estimates are often limited because of topographic blocking over mountainous watersheds and the uncertainty in the radar reflectivity versus rainfall rate ($Z-R$) relationship. Recent studies (Westrick and Mass 2001; Ibbitt et al. 2001; Jasper et al. 2002) show promising results of mesoscale meteorological modeling for predicting regional rainfall characteristics and the coupling of meteorological models with hydrological models for flood forecasting.

The purpose of this paper is to investigate the feasibility and uncertainty of simulating typhoon floods with a distributed hydrological model using both the observed rain gauge data and the predicted rainfall over a mountainous watershed in Taiwan. The Shihman Reservoir basin is the domain of interest in this study (Fig. 2). Our approach to simulating typhoon floods over this mountainous watershed is to perform physically based distributed hydrological modeling (FLO-2D; O'Brien et al. 1993) with rainfall forcings from gauge stations and a mesoscale meteorological model, the fifth-generation Pennsylvania State University–National Center for Atmospheric Research (PSU–NCAR) Mesoscale Model (MM5; Grell et al. 1994). The cases of Typhoons Zeb (1998) and Nari (2001) are selected for model calibration and validation, respectively. Observed river discharges are used to assess the performance of the predicted river discharge using this one-way-coupled hydrometeorological approach. Improved rainfall prediction by including the retrieved typhoon circulation from a single-Doppler radar for Typhoon Herb (1996) is then applied to further examine the predicted floods with the hydrological model (Chiang et al. 2001).

Brief descriptions of the hydrological and meteorological models, as well as the technique for assimilating radar-retrieved winds into a meteorological model, are discussed in section 2. Adapting the geographical description and the hydrometeorological data for this typhoon flood modeling are described in section 3. Synoptic overviews of the three typhoon events are presented in section 4, and the simulated typhoon flood responses are discussed in section 5. Conclusions and discussion are given in section 6.

2. Model descriptions

In this typhoon-flood study, the MM5-predicted rainfalls are applied to drive a distributed hydrological

model, FLO-2D (O'Brien et al. 1993), as well as the observed gauge data. The FLO-2D model is a Federal Emergency Management Agency (FEMA; U.S. Department of Homeland Security) approved hydraulic model for both river studies and unconfined flooding such as alluvial fan flows. It has been successfully applied to study the inundation potential of a mountainous watershed in central Taiwan (Li et al. 2002). The MM5 has worldwide usage in the mesoscale and microscale meteorology communities. It has been applied to investigate the rainfall characteristics and tracks of typhoons in Taiwan (Wu et al. 2002; Yang and Tung 2003). Both models are briefly introduced in the following subsections.

a. Hydrological model: FLO-2D

The FLO-2D model (O'Brien et al. 1993, 1998) is a physically based, distributed flood-routing model using the fully dynamic wave momentum equation and a central finite-difference routing scheme. River flow is described as a one-dimensional multiple channel network. Surface runoff is interpreted as a two-dimensional overland flow regime. The interactions between river flow and surface runoff can occur with overland return flow to the channel or as the overbank discharge when the flow exceeds channel capacity. Precipitation losses due to infiltration are described with the Green–Ampt (1911) infiltration model. Canopy interception is assigned as an initial abstraction factor. Infiltration and abstraction are combined as the total precipitation losses. More details of the model description and numerical algorithms can be found in O'Brien et al. (1998).

Model calibration is required to determine the most important spatially varied parameter (surface roughness) in channel flow and overland flow routings. The infiltration parameters of the Green–Ampt model are given at a grid base according to soil types of the study area. Reference values of these parameters for different soils are available in O'Brien et al. (1998). During model calibration, the roughness coefficients of the river network and surface grids are first estimated using the agrarian development indices of land-use maps as references. Then we adjust these roughness coefficients based on previous fitting results by examining the root-mean-square error (rmse) and goodness of fit (GOF) between the predicted and observed discharges in a trial-and-error procedure. The GOF is defined as $\Sigma(S_i - O_i)^2/S_p$, where S_i and O_i are the simulated and observed floods at the i th hour, respectively. The matching of high flow rate, to which the rmse value is sensitive, is very important because it mirrors the basin response of extreme events. However, a good correlation of the low flow rate, to which the GOF value is sensitive, should not be overlooked because the low flow part represents the overall performance of the hydrological model in capturing river flows and surface runoffs. The calibra-

tion procedure is ended if no further significant improvement of rmse and GOF values can be made.

b. Mesoscale meteorological model: MM5

The mesoscale meteorological model MM5 (Grell et al. 1994) is a three-dimensional, limited-area, primitive equation, nested-grid model with a terrain-following σ (nondimensional pressure) vertical coordinate. The physical parameterizations include the Grell (1993) subgrid-scale cumulus parameterization scheme, the Blackadar (1979) planetary boundary layer scheme, a radiation scheme with interaction between clear sky and clouds (Dudhia 1989), and a simple ice microphysics scheme (Dudhia 1989).

The initial and boundary conditions are taken from the European Centre for Medium-Range Weather Forecasts (ECMWF) analyses with 1.25° latitude \times 1.25° longitude horizontal resolution. The MM5 horizontal configuration includes three nested grids (with grid sizes of 60, 20, and 6.67 km) for Typhoon Zeb (1998), and four nested grids (with grid sizes of 60, 20, 6.67, and 2.22 km) for Typhoon Nari (2001), respectively. For the typhoon case of Herb (1996), Chiang et al. (2001) used the MM5 simulations of Wu et al. (2002) with nesting down to 2.22-km grid size and then assimilated the radar-retrieved winds into the MM5 fields. There are 31 σ levels in the vertical for all MM5 runs of three typhoons. Sea surface temperature is kept constant during the period of integration.

c. Assimilation of radar-derived winds

The application of weather radar data in extreme rainfall studies is shown to be useful for improving quantitative precipitation forecasting (Giannoni et al. 2003; Ganguly and Bras 2003; Zhang and Smith 2003). Chiang et al. (2001) enhanced the initial typhoon circulation with the retrieved wind field from a Weather Surveillance Radar-1988 Doppler (WSR-88D) at the Wu-Fen Mountain station in northeastern Taiwan (see Fig. 2) before Typhoon Herb (1996) made landfall. The data assimilation procedure of Chiang et al. (2001) is briefly described here. The typhoon circulation retrieval is based on the Ground-Based Velocity Track Display (GBVTD) technique (Lee et al. 1999). First, the horizontal circulation of Herb is derived from the single-Doppler radial winds using the GBVTD method. After transforming the retrieved typhoon wind from the height coordinate (for radar data) into the σ coordinate (for MM5), the derived typhoon winds are inserted into the original MM5-simulated winds, and a three-dimensional smoother is applied to remove discontinuities. Then the nonlinear balance equation is solved for the geopotential field from the wind field using an overrelaxation method. The hydrostatic equation is then used to obtain the corresponding temperature field. Once the horizontal wind, geopotential, and temperature fields are obtained, the inner domain of

MM5 is integrated forward with a small time step with fixed boundary conditions provided by the outer MM5 domain. The adjustment is done such that the MM5 fields inside the radar-observed region remain the same, and the MM5 fields outside the radar-observed region are gradually adjusted dynamically. Several iterations (normally 20 to 40 times) are required until the field outside the radar-observed region is converged. The MM5-predicted rainfalls with and without radar-derived wind assimilation are then used to drive the hydrological model for flood calculations, and they are also compared with those using the gauge forcing and observed flood discharges for Typhoon Herb (1996).

3. Geographical description and hydrometeorological data

a. Geographical description

The Shihmen Reservoir is located at the upstream of the Tamsui River basin (shown in the upper-right-hand side of Fig. 2) in northern Taiwan. In the absence of rapidly varied reservoir surface areas and depths during typhoon landfall periods, the Hsia-Yun stage station upstream of the Shihmen Reservoir is selected as the watershed outlet with a total drainage area of 622.8 km² (Fig. 2). Ten gauge stations (R1 through R10; see Fig. 2) provide ground-based rainfall data with an hourly resolution. The hourly discharge data at the Hsia-Yun station are used for hydrological model calibration and validation. The Digital Terrain Model (DTM) provides the surface elevations of this mountainous watershed (Fig. 3). Spatial land-use distribution of the Hsia-Yun watershed is given in Fig. 4, which shows that more than 94% of this watershed is covered by forest with mixed deciduous and coniferous trees. The soil classes of the watershed contain 39% sandy loam, 49% loam, and 12% sandy clay loam, which are used to determine the infiltration parameters for the Green-Ampt model.

b. Spatial data

The geographic information system (GIS) spatial analysis software named ArcView (Environmental Systems Research Institute 1996) is employed to perform geographic and hydrological data manipulations. By combining the corresponding GIS digital maps (watershed maps, river network maps, land-use maps, and DTM grids), the geographical, hydrological, and topographical data of the Hsia-Yun watershed is digitized for model applications. With a spatial resolution of 200 m \times 200 m, the target area is divided into 15 313 uniform-size grids. The coordinates and ground elevations of each grid are extracted from the DTM grids.

c. Hydrometeorological data

The wet season in northern Taiwan is from May to October. The major weather systems of mei-yu fronts

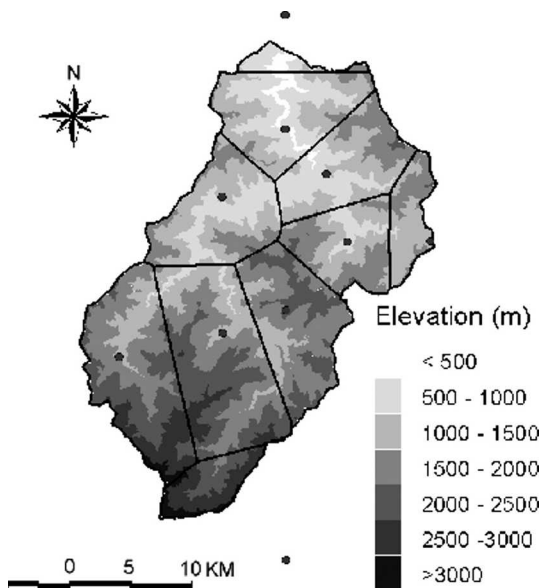


FIG. 3. Digital elevation map showing the surface elevations of the Hsia-Yun watershed and the Thiessen polygons (boundaries shown in black lines) generated for the corresponding gauge stations (shown in black dots).

(May and June) and typhoons (July to October) account for more than 60% of annual rainfall. From 1957 to 1999, the mean annual rainfall over the Shihmen Reservoir watershed was 2212 mm, the maximum annual rainfall was 3178 mm (in 1990), and the minimum

annual rainfall was 1277 mm (in 1964). Based on the 1963–2003 flow record, the maximum annual discharge at the Hsia-Yun station was 2826 mm (in 1990), the lowest discharge was 760 mm (in 1993), and the average annual flow was 1829 mm. The extreme maximum daily discharge was $6520 \text{ m}^3 \text{ s}^{-1}$ (i.e., 904 mm day^{-1}) on 11 September 1963 (associated with Typhoon Gloria). The recorded historical discharges show that the typhoon rainfalls are the major inputs of reservoir storage and the associated extreme floods for the Shihmen Reservoir. Rainfall gauge data are interpreted using the Thiessen (1911) polygons method to obtain basin-averaged rainfalls. The weighted area of each gauge station for the Hsia-Yun watershed is shown in Fig. 3.

4. Three typhoon events

a. Typhoon Zeb (1998)

The Mongolia high pressure that develops over the east Asian continent becomes progressively stronger and affects the weather in Taiwan from mid-September to April in the following year, as the Mongolia high pressure circulation is dominant over the continent. When a tropical cyclone moves toward Taiwan from the western Pacific Ocean, the northeasterly wind over Taiwan may be enhanced due to the “coupled circulation” between the northeasterly wind associated with the Mongolia high-pressure circulation and the northeasterly wind associated with the outer cyclonic circulation of a typhoon. This situation often results in heavy

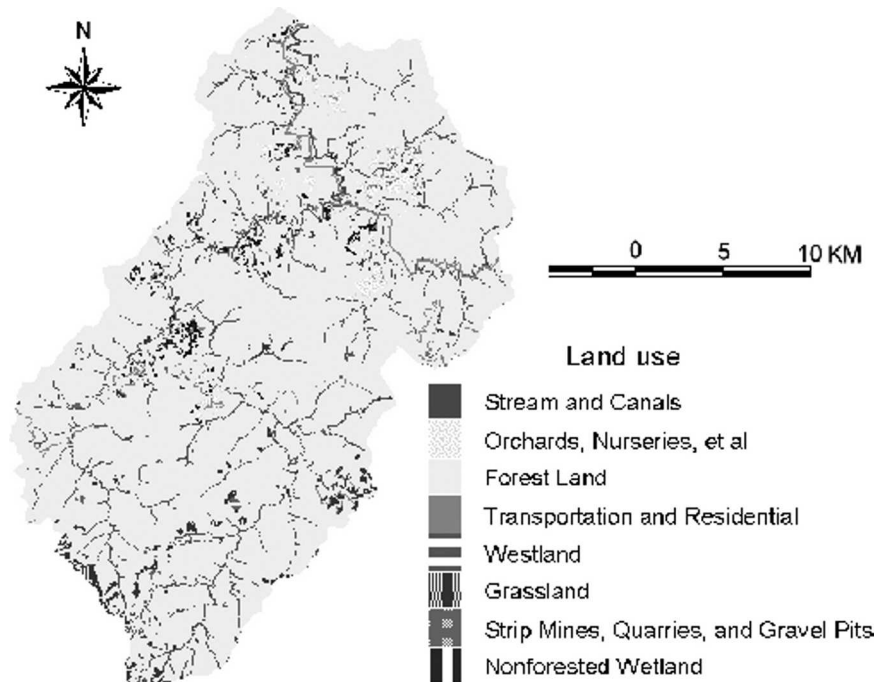


FIG. 4. Spatial land-use distribution for the Hsia-Yun watershed.

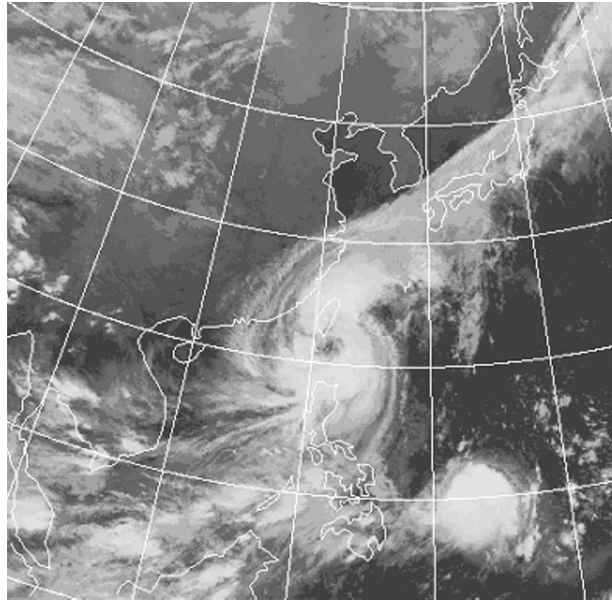


FIG. 5. The IR satellite map at 1200 UTC 15 Oct 1998 for Typhoon Zeb.

rainfall and strong gusty winds over northern and northeastern Taiwan during a typhoon's landfall period. The satellite image (Fig. 5) of Typhoon Zeb at 1200 UTC 15 October 1998 shows the clear eye structure of Zeb, the anvil clouds associated with Zeb's upper-level outflows, and a long cold-frontal cloud band associated with the Mongolia high pressure circulation. Although Typhoon Zeb (1998) moved along the east coast of Taiwan without making landfall (Fig. 6), the interaction of the typhoon circulation and mountainous terrain brought heavy rainfall over eastern and northern Taiwan (see Fig. 7). The corresponding MM5-predicted track from 0000 UTC 15 October to 0000 UTC 17 October 1998 is shown in Fig. 6. The mapping of the finest MM5 6.67-km grid (shown in black dots) onto the Hsia-Yun watershed and the associated weighted area for each grid is shown in the left panel of Fig. 8. The basin-averaged rainfall hyetographs estimated from the rain gauge data and the MM5-predicted rainfall are given in Fig. 9. The observed rainfall peaks were 27.5 mm h^{-1} (at the model time of hour 21) and 42.1 mm h^{-1} (at the model time of hour 37). On the other hand, the MM5-predicted rainfall peaks are 33.7 mm h^{-1} (at the model time of hour 17) and

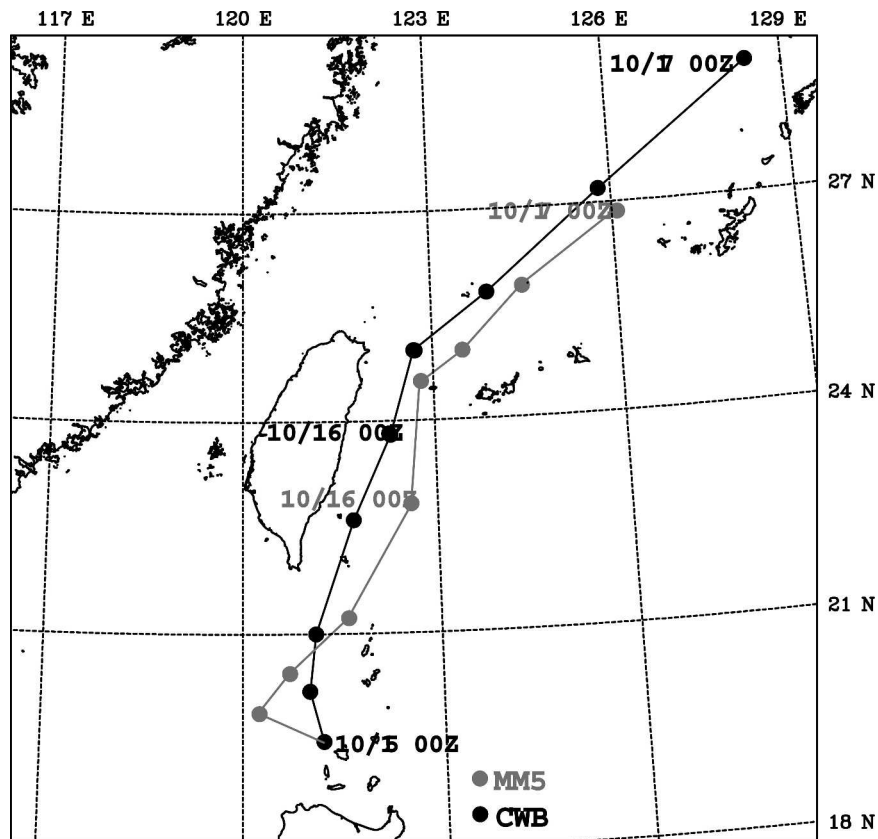


FIG. 6. Tracks of Typhoon Zeb reported from the CWB (shown in black line with circles for every 6 h) and MM5 run (shown in gray line with circles every 6 h) from 0000 UTC 15 Oct to 0000 UTC 17 Oct 1998.

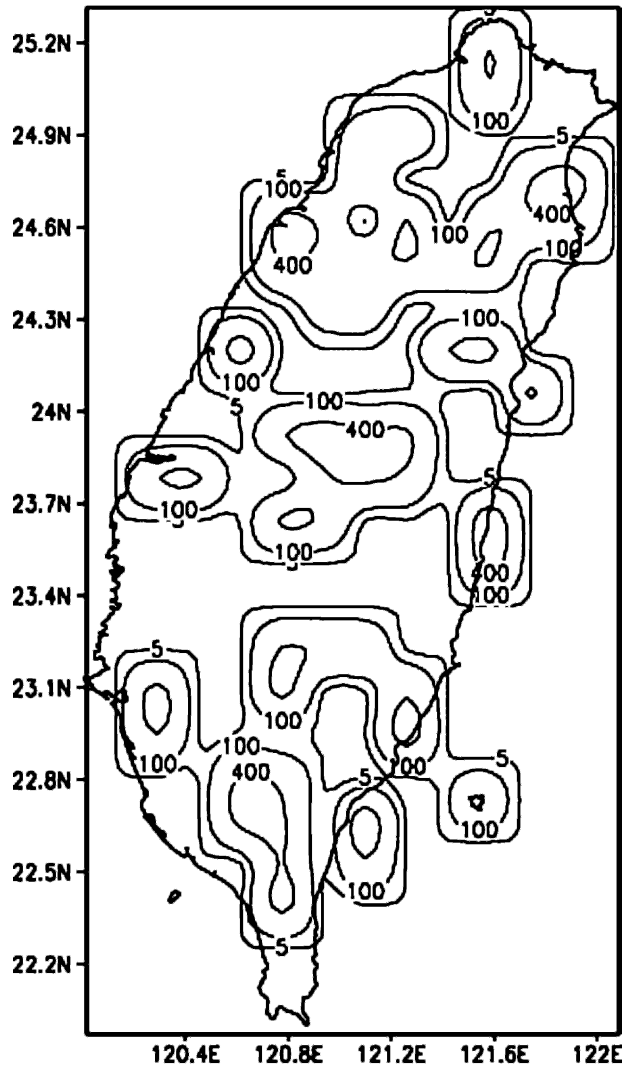


FIG. 7. Horizontal distribution of 54-h accumulated rainfall (mm) from 1800 UTC 14 Oct to 0000 UTC 17 Oct 1998 for Typhoon Zeb. Rainfall is contoured at 5, 100, and 400 mm.

49.2 mm h⁻¹ (at the model time of hour 38), with relative peak errors of 23% and 17%, respectively.

b. Typhoon Nari (2001)

Typhoon Nari (2001) broke several hydrometeorological records and was the typhoon that produced the most severe damage over Taiwan in the recent century. This typhoon grew from a category 1 tropical cyclone on 6 September 2001 between Okinawa, Japan, and Taiwan, and passed four times over an area about 500 km² to the northeast of Taiwan for 8 days. Until 16 September 2001, the high pressure over east Asia resulted in a northeasterly steering flow and advected the typhoon southwestward toward the island of Taiwan. After making landfall over the northeastern Taiwan at 1400 UTC 16 September 2001 (Fig. 10), Typhoon Nari

moved slowly across the island for 49 h, until the typhoon center moved into the Taiwan Strait at 1500 UTC 18 September 2001. The maximum surface wind over Taiwan was only 40 m s⁻¹. However, severe flooding damage was caused by such a long period of heavy rainfall.

The record-breaking 24–48-h accumulated rainfall of 1000 mm over northern Taiwan (Fig. 11) was associated with high ocean temperature, the slow-moving typhoon, and the island's steep terrain (Sui et al. 2002). The tremendous rainfall overwhelmed the existing flood control capacity and inundated more than 500 buildings and the underground subway (Mass Rapid Transport) system in Taipei, the largest city downstream of the Tamsui River basin. In addition to the official track of Typhoon Nari from the Central Weather Bureau (CWB), the MM5-predicted track is shown in Fig. 10. Details of the MM5 simulation of Typhoon Nari can be found in Yang and Huang (2004). It is clear in Fig. 10 that Typhoon Nari's track is well predicted by the MM5. The mapping of the finest MM5 2.22-km grids onto the Hsia-Yun watershed is shown in the center panel of Fig. 8 with the associated weighted area of each grid for interpreting the basin hyetograph. The basin-averaged rainfall rates estimated from the gauge data and the MM5 model for Typhoon Nari are given in Fig. 12. The observed rainfall peaks were 37.6 mm h⁻¹ (at the model time of hour 47) and 35.4 mm h⁻¹ (at the model time of hour 65). For comparison, the MM5-predicted rainfall peaks are 58.8 mm h⁻¹ (at the model time of hour 47, the same as the observed peak time) and 34.0 mm h⁻¹ (at the model time of hour 67). It is clear that the MM5 perfectly predicted the timing of the first rainfall peak, with a 56.5% overestimation of peak amount, and MM5 had a slight (2 h) timing delay of the second rainfall peak with minor (4%) underestimation of peak amount.

c. Typhoon Herb (1996)

Supertyphoon Herb struck northern Taiwan from 1400 UTC 31 July to 2000 UTC 31 July 1996. Although the landfall period was short, the associated extensive rainfall and gusty winds induced severe floods in northern Taiwan and mudslides in central Taiwan. The topographical effects on the rainfall amounts and distribution for Typhoon Herb (1996) were investigated by Wu et al. (2002). The mapping of the MM5 6.67-km grids on the Hsia-Yun watershed is shown in the right panel of Fig. 8 with the associated weighted area of each grid.

The purpose of including this typhoon event in this study is to compare the simulated floods without radar data assimilation (Wu et al. 2002) and with radar data assimilation (Chiang et al. 2001). Since we are interested in the effect of an improved typhoon prediction on rainfall estimates during peak periods, the MM5-predicted rainfall is taken in a period of 6 h with radar

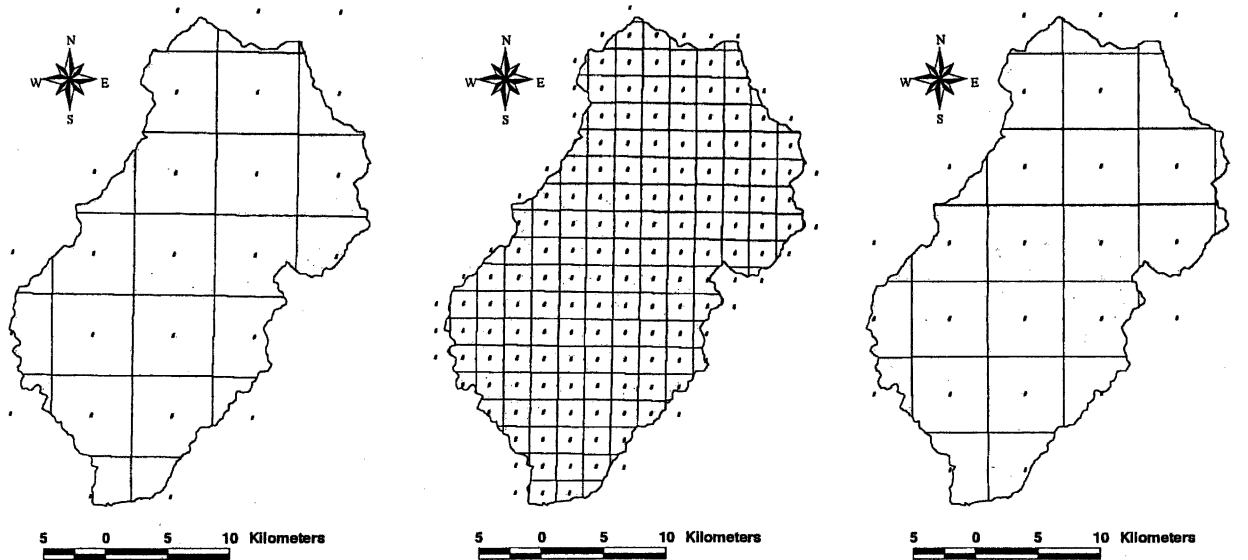


FIG. 8. Mapping of the MM5 grid points (shown in black dots) onto the Hsia-Yun watershed for Typhoons (left) Zeb, (center) Nari, and (right) Herb.

data assimilation and in a period of 18 h without the assimilation (Fig. 13). For the compatibility in hydrological modeling with gauge data forcing, rainfall over periods before and after the MM5-predicted rainfall is specified to be the gauge values. The basin-averaged rainfall hyetographs estimated from gauge data and two MM5 runs are given in Fig. 13. The observed rainfall peak was 48.0 mm h^{-1} (at the model time of hour 37). The original MM5 rainfall peak was 112.4 mm h^{-1} (at the model time of hour 38), and the radar-improved MM5 rainfall peak was 76.3 mm h^{-1} (at the model time of hour 38). Although both MM5 runs produced over-estimated rainfall peaks, the MM5-predicted rainfall with assimilated radar-retrieved wind greatly reduced

the rainfall peak without introducing any additional phase error.

5. Typhoon flood responses

Using a trial-and-error process, the roughness coefficients of the domain are calibrated using gauge data of Typhoon Zeb to drive the FLO-2D model. Once these spatially varied surface roughness coefficients, treated as event-independent parameters, are obtained in the calibration step, they are fixed in other typhoon simulations for verifications (Typhoons Nari and Herb) and comparisons (the MM5-predicted rainfall). Table 1 is a

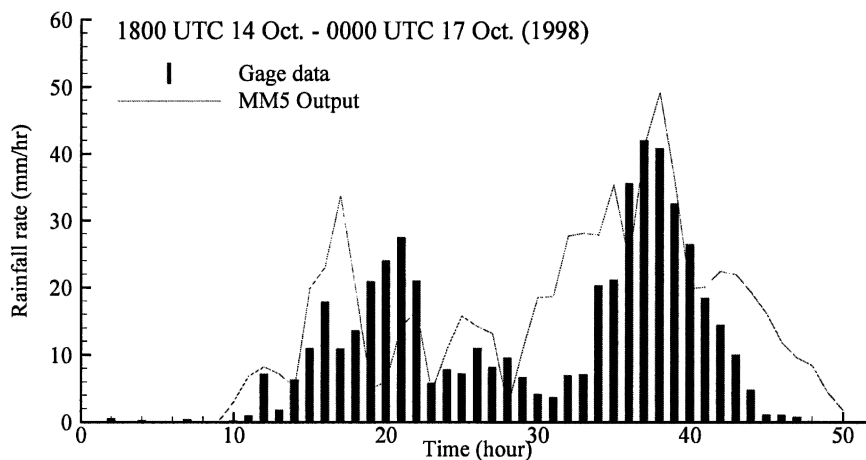


FIG. 9. Basin-averaged rainfall rate estimated from the gauge data and the MM5 simulation for Typhoon Zeb.

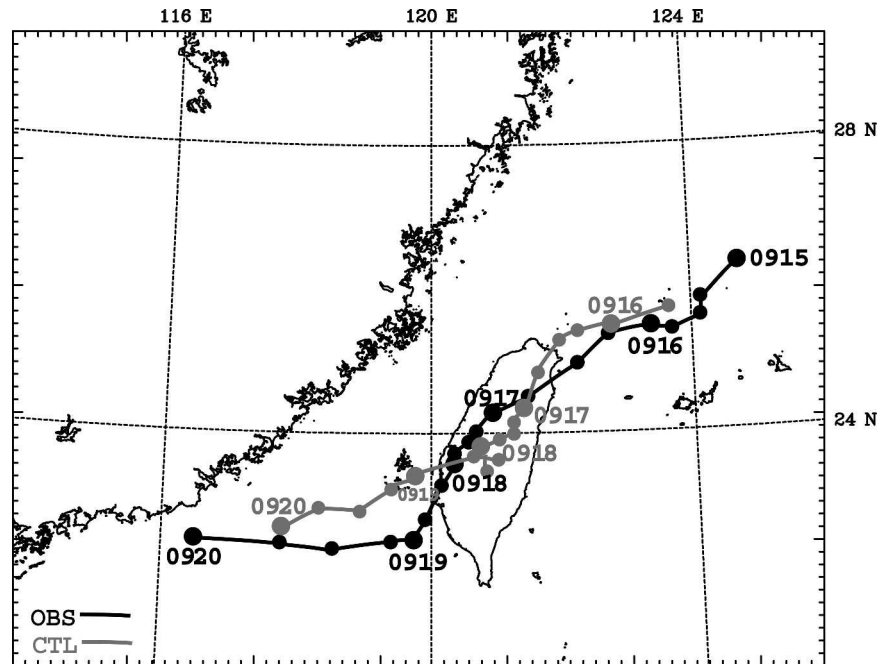


FIG. 10. Tracks of Typhoon Nari reported from the CWB (shown in black line with circles for every 6 h; 0000 UTC 15 Sep to 0000 UTC 20 Sep 2001) and predicted by MM5 run (shown in gray line with circles every 6 h; 1800 UTC 15 Sep to 0000 UTC 20 Sep 2001).

list of the observed and simulated flood responses with gauge data and the MM5-predicted rainfall focusing on predicted flood peaks and time lags for the three typhoon events. Discussion for each typhoon event is presented in the following subsections.

a. Typhoon Zeb (1998)

The observed and predicted flood hydrographs at the Hsia-Yun Station for Typhoon Zeb are given in Fig. 14. The two distinctive rainfall peaks in Fig. 9 lead to two basin discharge peaks of 1301 and $3715 \text{ m}^3 \text{ s}^{-1}$, respectively. Since this typhoon event was used to calibrate the hydrological model with the gauge data, the best-predicted discharge peaks were 953 and $3647 \text{ m}^3 \text{ s}^{-1}$, with time lags of -2 and $+1$ h (“ $-$ ” means an early arrival and “ $+$ ” means a late arrival), respectively. The first flood peak is underestimated, which is probably caused by the overestimates of initial precipitation losses, including both infiltration and abstraction. The second flood peak was successfully simulated with a relative peak error of 2%. The timing errors of both simulated peaks (± 2 h) after this calibration with gauge data would be quite acceptable for hydrological applications.

The predicted flood peaks with the MM5-predicted rainfalls were 807 and $4961 \text{ m}^3 \text{ s}^{-1}$, with time lags of -5 and $+2$ h, respectively. Note that there is another peak of $1147 \text{ m}^3 \text{ s}^{-1}$ with a time lag of $+5$ h with the MM5 forcing for the first flood peak. The underestimate of the first flood peak with the MM5 rainfall forcing is

caused by the timing phase error in the MM5-predicted rainfall (Fig. 9). The phase error of the first rainfall peak also plays a role in attenuating the first flood peak with a large time lag in return. Although the time lag of the second peak with the MM5 forcing is acceptable, the relative peak error of predicted flood is 34%. As discussed in section 4a, the relative errors of the two MM5 rainfall peaks are 23% and 17%, with time lags of -4 and $+1$ h, respectively. While the relative error of the first rainfall peak is higher than that of the second one, the skill of the resultant flood responses is the opposite. This implies that the flood responses over the mountainous watershed are highly sensitive to extreme rainfall predictions.

b. Typhoon Nari (2001)

The observed and predicted flood hydrographs at the Hsia-Yun Station for Typhoon Nari (2001) are given in Fig. 15. Similar to the Zeb event, there are two distinctive rainfall peaks for Nari as well (Fig. 12), and the two corresponding flood peaks are 2439 and $2639 \text{ m}^3 \text{ s}^{-1}$. Using the hydrological parameters calibrated by Typhoon Zeb, the simulated flood peaks with gauge data for Typhoon Nari are 2316 and $2375 \text{ m}^3 \text{ s}^{-1}$, with time lags of $+2$ h for both flood peaks. The relative peak flood errors are 5% and 10%, respectively. These results with observed rainfall demonstrate the successful application of a physically based distributed hydrological model for simulating typhoon floods in a mountainous watershed.

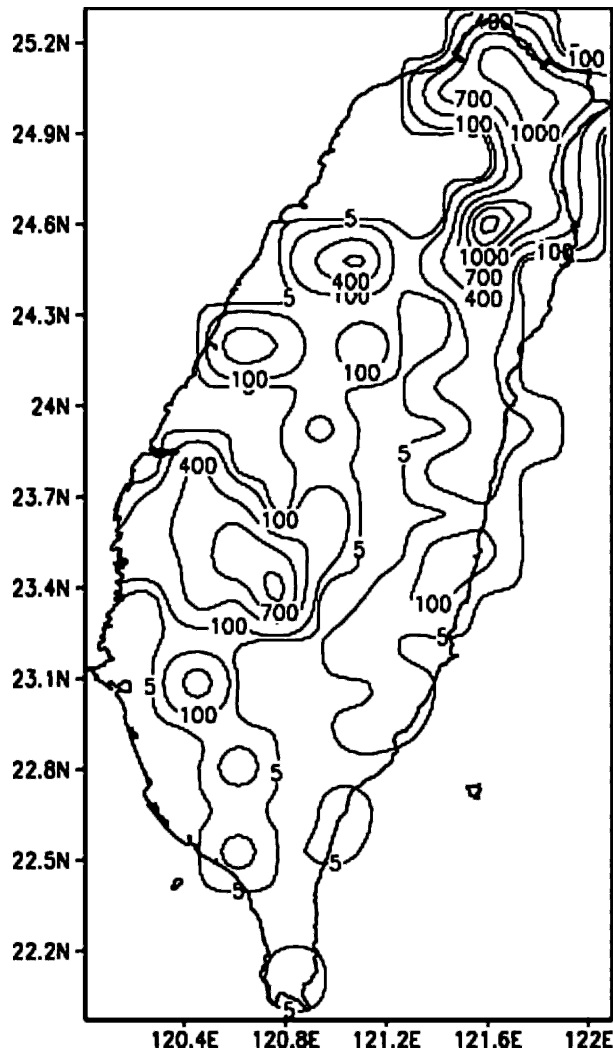


FIG. 11. Horizontal distribution of 93-h accumulated rainfall (mm) from 1800 UTC 14 Sep to 1500 UTC 18 Sep 2001 for Typhoon Nari. Rainfall is contoured at 5, 100, 400, 700, 1000, 1200, and 1400 mm.

The predicted flood peaks with the MM5 rainfall forcing (Fig. 15) were 4306 and $3095 \text{ m}^3 \text{ s}^{-1}$ with time lags of +5 and +0 h, respectively. Note the curious predicted twin peaks for the second flood peak hydrograph around model time hour 70. However, the major focus of this discussion will be on the first flood peak, since the relative errors of flood peaks are 77% and 17%, respectively. These predicted flood peaks are directly related to the corresponding relative errors in the MM5 rainfall peaks of 56% and 4% (Fig. 12). The large error of the first peak demonstrates that the flood response is fast and the error in the rainfall estimate may be significantly amplified in the mountainous watershed owing to persistent intensive rainfall and steep terrain slopes. Whereas the time lag of the MM5-predicted first rainfall peak is +2 h, there is no time lag for the predicted second flood peak. This discrepancy may be due to the overestimated low rainfalls between two peaks and the large phase error of the first predicted rainfall peak by the MM5 (Fig. 12).

c. Typhoon Herb (1996)

The observed and predicted flood hydrographs for Typhoon Herb (1996) are presented in Fig. 16. The simulated hydrographs by the MM5 forcing have been supplemented with the gauge data before and after available rainfall peak periods, as described in section 4c. The main reason to include this typhoon event in this study is to analyze the improved flood responses for the MM5 run with assimilated radar data. The observed flood peak is $5084 \text{ m}^3 \text{ s}^{-1}$. The simulated peak with gauge data is $5109 \text{ m}^3 \text{ s}^{-1}$ with a time lag of +1 h, so that the relative peak error is only 0.5%. The predicted flood peaks with rainfall inputs from the original MM5 and the radar-data assimilated MM5 are $10\,470 \text{ m}^3 \text{ s}^{-1}$ (with +2 h time lag) and $8482 \text{ m}^3 \text{ s}^{-1}$ (with -1 h time lag), respectively. With the better rainfall prediction from assimilating radar-derived winds into the

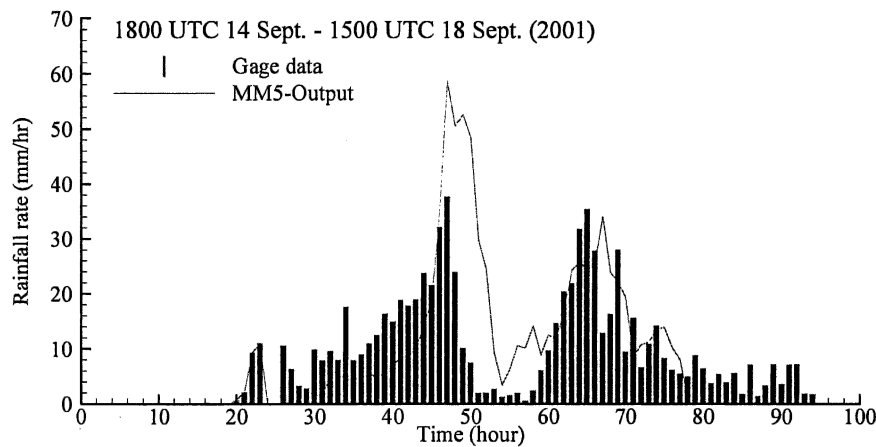


FIG. 12. Basin-averaged rainfall rate estimated from the gauge data and the MM5 simulation for Typhoon Nari.

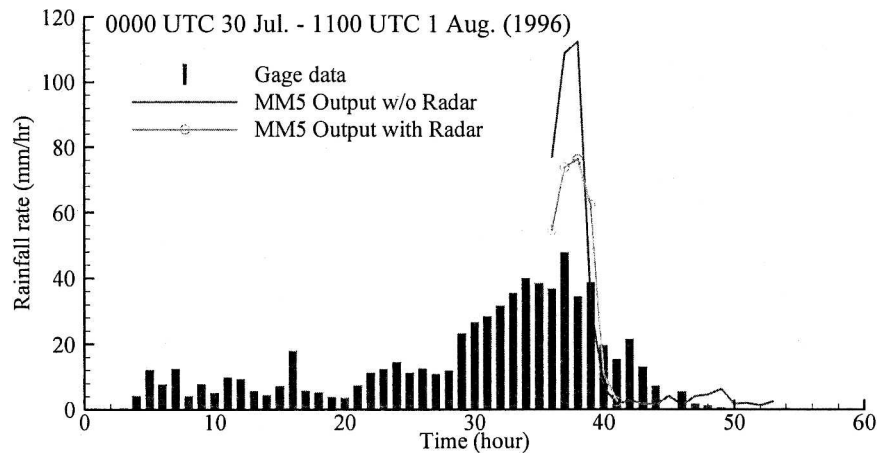


FIG. 13. Basin-averaged rainfall rate estimated from the gauge data and the MM5 simulations with and without radar data assimilations for Typhoon Herb.

MM5 fields, the relative peak error of the predicted flood is reduced from 106% to 67%, which is mainly attributed to the reduction of predicted rainfall peak from 112.4 mm h^{-1} (with +1 h time lag) to 76.3 mm h^{-1} (with +1 h time lag). This result suggests a promising potential of integrating Doppler radar observations and mesoscale-modeled rainfalls for typhoon rainfall forecasts and the subsequent hydrological applications.

d. Runoff ratio

In the above discussion, only the relative errors of simulated flood peaks and time lags have been analyzed. To better understand the skill of this integrated hydrometeorological approach for typhoon flood forecasts, the predictions for each typhoon event are further investigated by calculating the runoff ratio (RR), which is defined as the ratio of observed (or predicted) flood over the corresponding rainfall forcing, either gauge data or the MM5-predicted rainfall. The rmse and GOF values of three events are compared to evaluate the overall performance of each prediction. Table 2 is the summary of these comparisons for the three typhoon floods. Note that the total hydrologic model time with the MM5 data are 13 h (Typhoon Nari) and 6 h (Typhoon Herb) shorter than that with gauge data, as shown in Figs. 15 and 16, respectively.

The flood simulations with the observed rainfall data have the highest RR values compared to the simula-

tions with the rainfall forcing from the MM5 runs for all three events. The low RR values with gauge data are caused by the underestimates of total floods, which contribute significantly to the errors in predicting the falling limb of flood hydrographs (Figs. 14, 15, and 16). The RR values with the MM5 rainfall forcing are better than those with the gauge data and are close to the RR values with the observed rainfall. The MM5 rainfall estimates are usually too large with timing phase errors for the three flood events. The excessive rainfall may be because the MM5-predicted typhoon tracks are closer to the basin area than in observations (see Figs. 6 and 10). The computed flood responses are persistently higher than the observed data as well as for the falling limb of hydrographs, which are poorly predicted by the hydrological model using gauge data forcing. Note that the first rising limb is underestimated by the MM5 forcing, so the apparent phase and peak errors of the first predicted flood peak overcompensate for the insufficient rising floods.

Although the RR values of the MM5 forcing are superior to the gauge data, the rmses with the gauge data forcing are 2.35 mm for Typhoon Zeb (1998), 1.86 mm for Typhoon Nari (2001), and 2.35 mm for Typhoon Herb (1996), respectively. With the MM5-predicted rainfall, the rmses are much higher than those using the gauge data. Similar results are also found in GOFs. Note that the GOF for the prediction with MM5 forcing

TABLE 1. Comparisons of peak discharge (Q_p ; $\text{m}^3 \text{ s}^{-1}$) between the observed and the simulated results with gauge data (Q_{pg}) and with MM5 runs (Q_{pM}) and time lag (hour) of peak discharge for Typhoons Zeb, Nari, and Herb. Positive/negative time lag indicates simulated peak discharge is later/earlier than the observed.

Typhoons	Q_p		Q_{pg} (time lag)		Q_{pM} (time lag)	
Zeb	1301	3715	953 (-2)	3647 (+1)	807 (-5)	4961 (+2)
Nari	2439	2639	2316 (+2)	2375 (+2)	4306 (+5)	3095 (0)
Herb	5084			5109 (+1)	10 470 (+2)	8482 (-1)

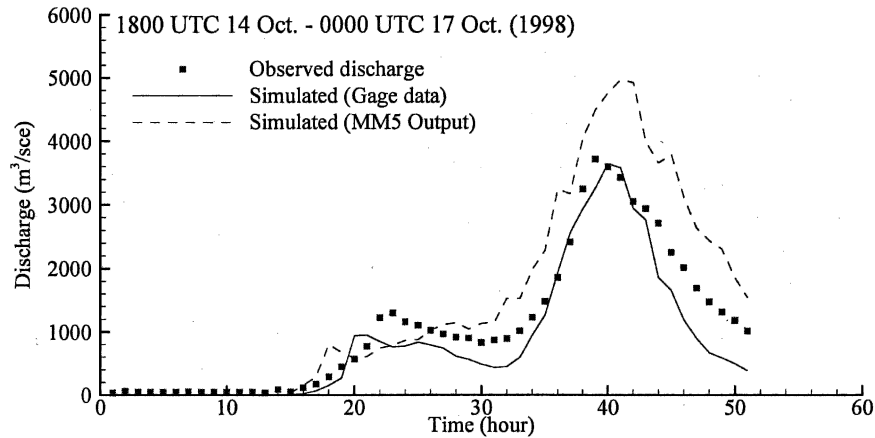


FIG. 14. Simulated and observed hydrographs for Typhoon Zeb.

for Typhoon Nari are much higher than the other two cases, which are caused by the substantial phase and peak errors in predicting the first flood peak (Fig. 15).

e. Spatial distribution of typhoon rainfall and flood

The spatial distribution of rainfall presented in this subsection contains rainfall fields of the Thiessen polygon interpolated from gauge data (upper panel of Figs. 17, 18, and 19) and the mapping grids of the MM5-predicted rainfall (center panel of Figs. 17, 18, and 19) for Typhoon Zeb, Nari, and Herb, respectively. The spatial distribution of flood is given as the simulated water depths (bottom panel of Figs. 17, 18, and 19) at the specific hours corresponding to the cumulated periods of spatial rainfall depicted. Since there is no observed spatial distribution of flood depths, the results presented herein are used to demonstrate the spatial characteristics of flood captured by the hydrologic model.

For Typhoon Zeb, the first cumulated period (1800

UTC 14 October to 1300 UTC 15 October; left panel of Fig. 17) contains the first rainfall peak (see Fig. 9), in which the MM5-predicted rainfall is underestimated. The second cumulated period (1800 UTC 14 October to 0400 UTC 16 October; left panel of Fig. 17) contains both rainfall peaks of Typhoon Zeb (see Fig. 9), in which the MM5-predicted overall rainfall is overestimated. Higher rainfall intensity is found in the east of the domain, and rivers at the east and north (downstream) have higher water depths as simulated by the hydrological routing.

For Typhoon Nari, the first cumulated period (1800 UTC 14 September to 1600 UTC 16 September; left panel of Fig. 18) contains the first rainfall peak (see Fig. 12), in which the MM5-predicted rainfall is underestimated. The second cumulated period (1800 UTC 14 September to 1000 UTC 17 September; left panel of Fig. 18) contains both rainfall peaks of Typhoon Nari (see Fig. 10), in which the MM5-predicted overall rainfall is overestimated. Higher rainfall intensity is found in the north of the domain, and rivers at the north have

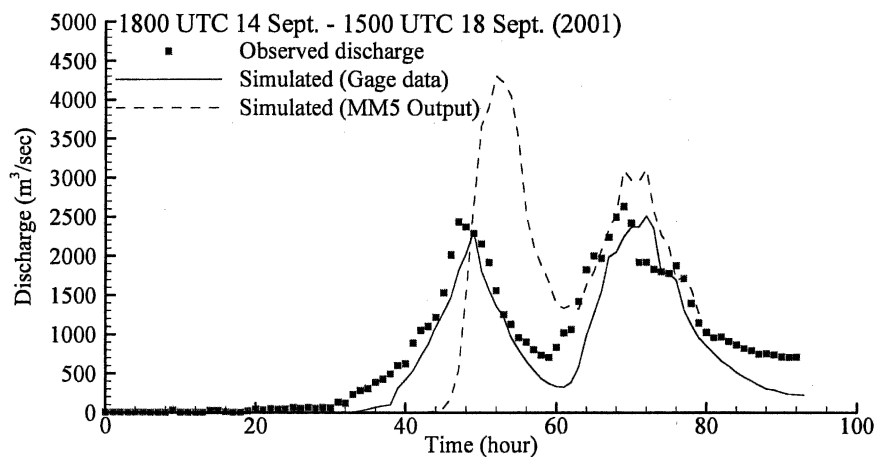


FIG. 15. Simulated and observed hydrographs for Typhoon Nari.

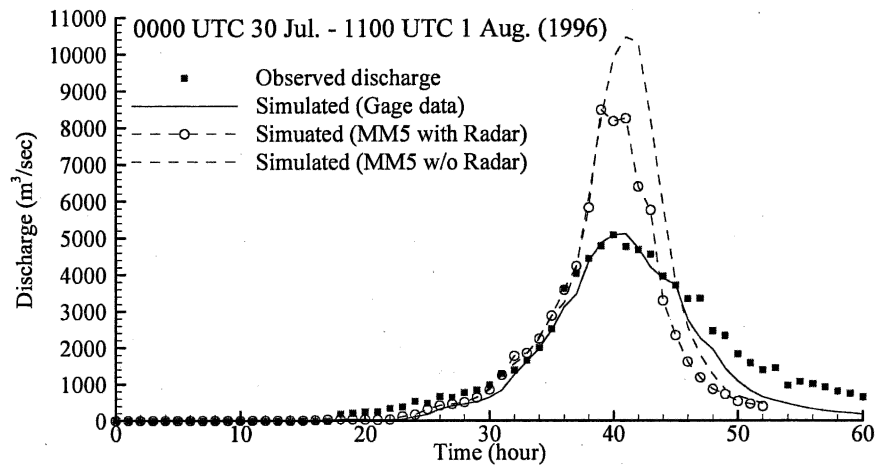


FIG. 16. Simulated and observed hydrographs for Typhoon Herb.

higher water depths as simulated by the hydrological routing.

For Typhoon Herb, the first cumulated period (0000 UTC 30 July to 1300 UTC 31 July; left panel of Fig. 19) contains the first rainfall peak (see Fig. 13), in which the MM5-predicted rainfall is overestimated over most of the domain. The second cumulated period (0000 UTC 30 July to 1800 UTC 31 July; left panel of Fig. 19) contains the major rainfall of Typhoon Herb (see Fig. 10), in which the MM5-predicted overall rainfall is overestimated. Higher rainfall intensity is found in the southwest and north of the domain, and rivers at the north have higher water depths as simulated by the hydrological routing.

6. Conclusions and discussion

A one-way-coupling approach between a mesoscale meteorological model (MM5) and a physically based

distributed hydrological model (FLO-2D) has been conducted to simulate the flooding events of three typhoons (Zeb, Nari, and Herb) over a mountainous watershed in Taiwan. This small number of typhoon cases and great event-to-event variability pose a strong limitation of conclusions reached in this study. However, the physical insights found in this paper might be applicable to other typhoon (or hurricane) cases with similar tracks and intensities and over watersheds with comparable sizes and terrain slopes.

Since this study is a one-way forcing approach, the rainfall hyetographs predicted by the MM5 integrations play an essential role on the subsequent flood predictions. With a horizontal resolution of 2.22 km, MM5 may be able to successfully simulate the typhoon track and to capture the island-wide rainfall characteristics for the typhoon events. However, this 2.22-km grid resolution is still not able to resolve the detailed rainfall distribution in a small watershed with complex terrain.

TABLE 2. Comparisons of total flood (Q), total rainfall (P), and the runoff ratio ($RR = Q/P$) of the observed data and simulated results with gauge data and MM5 rainfall estimates for Typhoons Zeb, Nari, and Herb. The rmse and GOF are computed with observed and predicted flood hydrographs (Q , P , rmse, and GOF are all in units of mm).

	Observed data	Gauge data	MM5 rainfall estimates	
Zeb	$Q = 357$ $P = 516$ RR = 0.69	$Q = 267$ $P = 516$ RR = 0.52 Rmse = 2.35 GOF = 279.0	$Q = 443$ $P = 703$ RR = 0.63 Rmse = 4.13 GOF = 173.7	
Nari	$Q = 455$ $P = 782$ RR = 0.58	$Q = 350$ $P = 782$ RR = 0.45 Rmse = 1.86 GOF = 445.7	$Q = 459$ $P = 816$ RR = 0.56 Rmse = 5.20 GOF = 6407.0	
Herb	$Q = 487$ $P = 696$ RR = 0.70	$Q = 396$ $P = 696$ RR = 0.57 Rmse = 2.35 GOF = 154.4	Original MM5 $Q = 543$ $P = 870$ RR = 0.62 Rmse = 9.05 GOF = 197.2	With radar data $Q = 446$ $P = 728$ RR = 0.61 Rmse = 6.06 GOF = 196.0

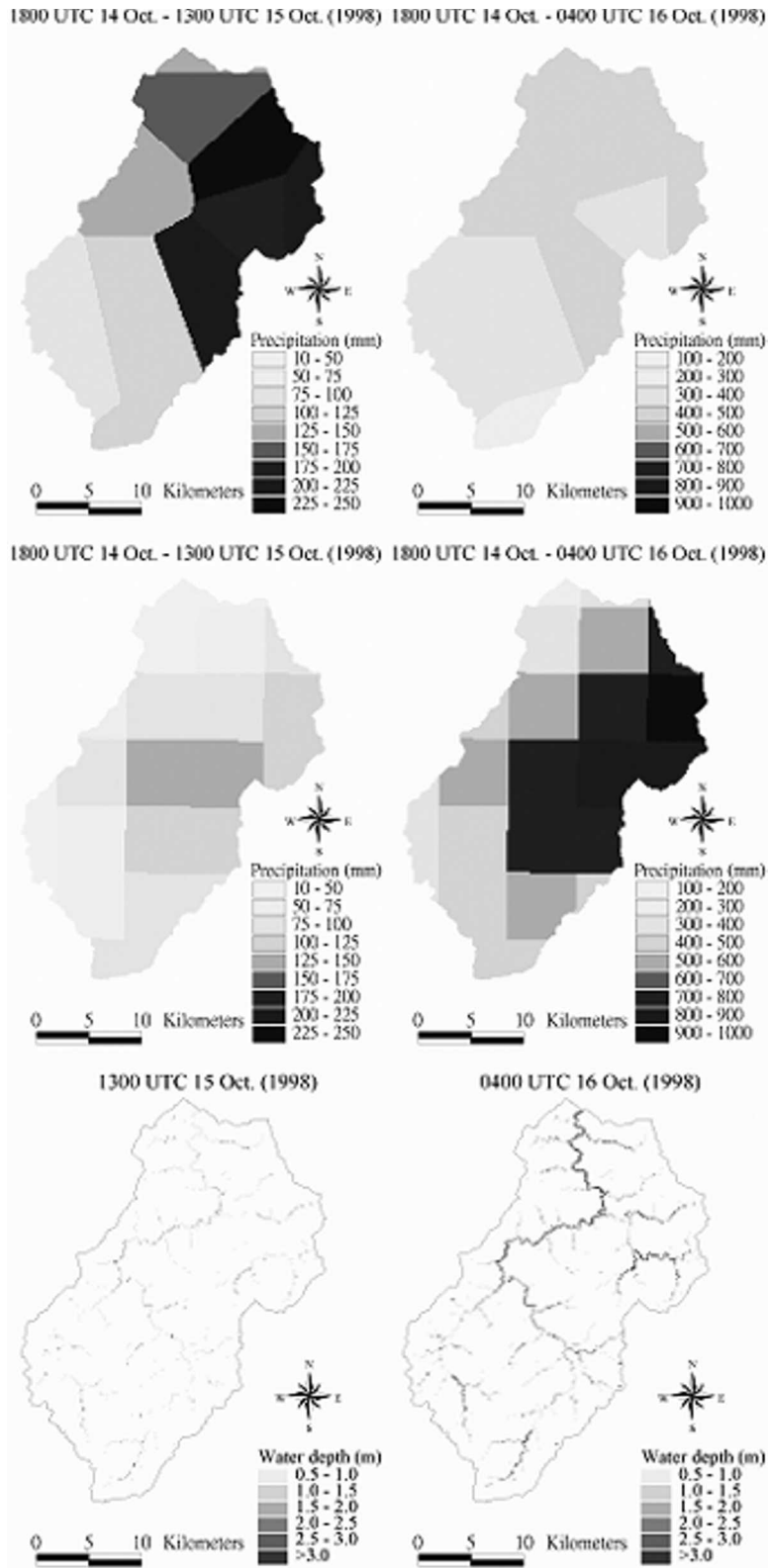


FIG. 17. The cumulated spatial rainfall for the Thiessen polygons from (top) gauge data and (center) the MM5 grids, and (bottom) the simulated flood water depths with the Thiessen polygon rainfall for Typhoon Zeb.

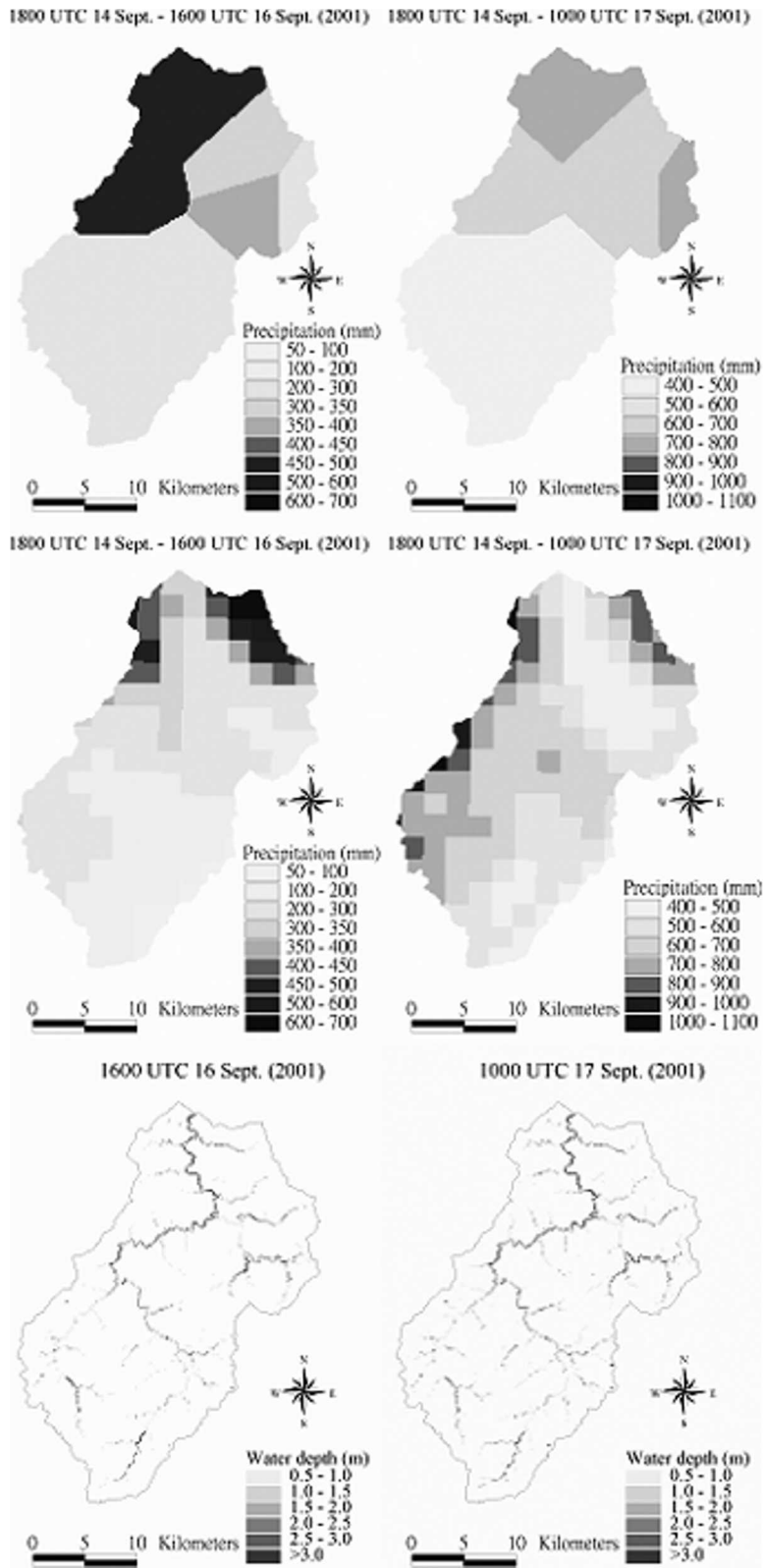


FIG. 18. The cumulated spatial rainfall for the Thiessen polygons from (top) gauge data and (center) the MM5 grids, and (bottom) the simulated flood water depths with the Thiessen polygon rainfall for Typhoon Nari.

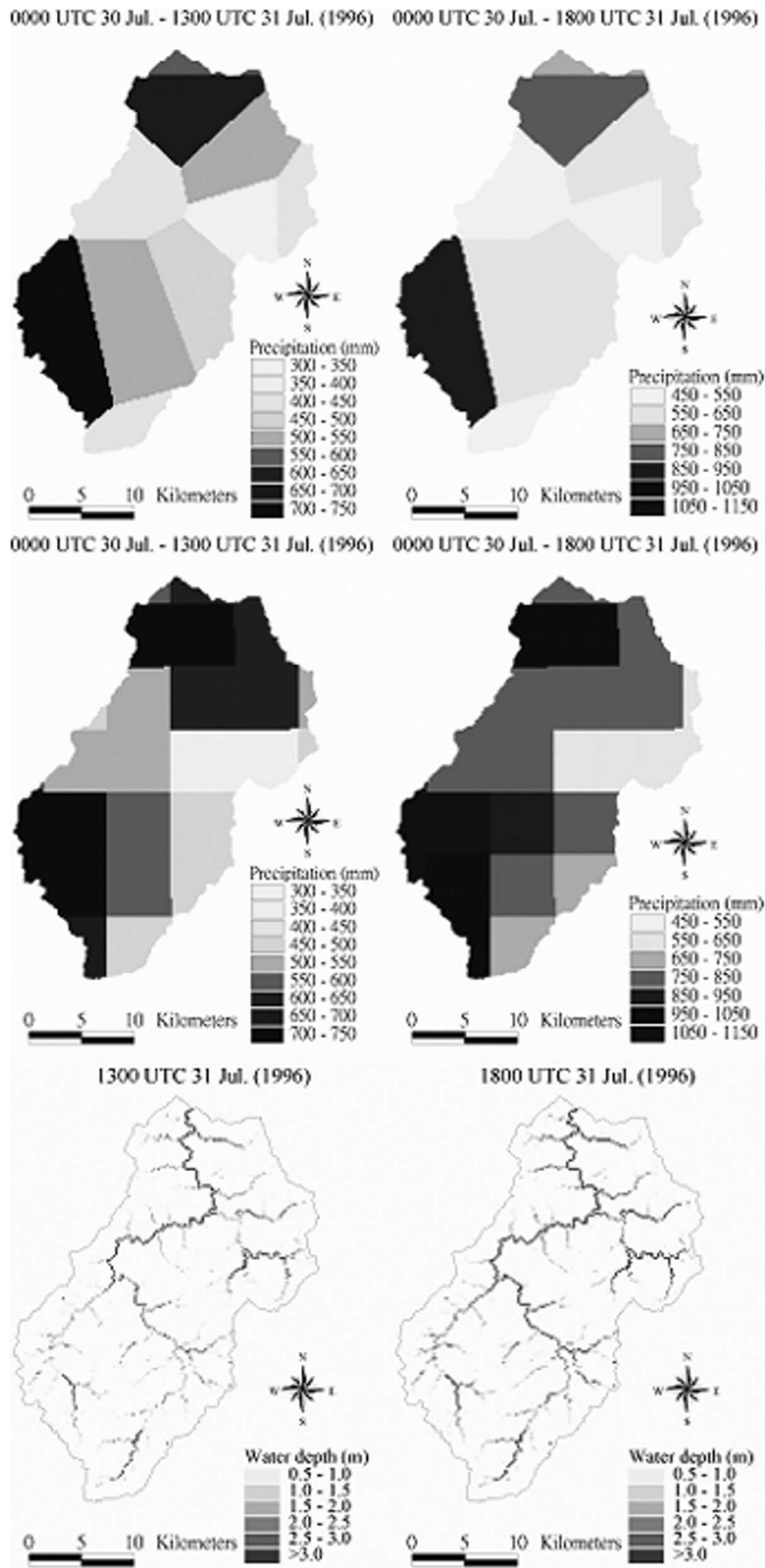


FIG. 19. The cumulated spatial rainfall for the Thiessan polygons from (top) gauge data and (center) the MM5 grids without radar data, and (bottom) the simulated flood water depths with the Thiessan polygon rainfall for Typhoon Herb.

The predicted flood hydrographs with gauge data are in good agreement with the observations in terms of peaks and time lags for all three flood events. The typhoon flood response over this mountainous watershed occurs rapidly and has high flood peaks. The MM5-predicted rainfall hyetographs for this mountainous watershed are overestimated with some timing errors for three typhoon flood events. The simulated flood hydrographs significantly amplify such discrepancies in rainfall predictions owing to the fast basin flood responses.

The hydrological model skill in predicting the falling limb of flood hydrographs is limited, probably because of the neglect of the return flow from saturated groundwater. Other sophisticated hydrological models, such as the Distributed Hydrology Soil Vegetation Model (DHSVM; Wigmosta et al. 1994), consider the return and saturation overland flow. Thus these hydrological models may be able to better describe the falling limb. In this study, the overall skill of the hydrological model is acceptable as the computed rmse are less than 2.5 mm for the three typhoon events, with the total floods ranging from 357 mm for Typhoon Zeb (1998) to 487 mm for Typhoon Herb (1996).

Typhoon floods are one of the major natural hazards that frequently cause societal and economical damages in Taiwan. For better flood mitigation, it is a necessity to conduct the interdisciplinary hydrometeorological research. The fast flood response over the mountainous watershed can only be successfully forecasted when the rainfall is accurately predicted. This one-way-coupling hydrometeorological study clearly illustrates that future improvement of flood forecasts mainly relies on the progress in rainfall predictions by mesoscale meteorological models. The different spatial resolutions between the meteorological and hydrological model may become an important limiting factor for long-period hydrological simulations when the two-way land-atmosphere interactions dominate the hydrological cycles. For typhoon flood predictions over a mountainous watershed such as in Taiwan, this one-way coupling might be an acceptable and applicable approach. More case studies are required to further examine the feasibility of this one-way-coupled hydrometeorological approach for typhoon flood events.

Acknowledgments. This study is supported by the National Science Council of Taiwan through the National Central University under Grants NSC-91(92)-2621-Z-008-009 and NSC 92-2625-Z-008-012. Valuable hydrometeorological data were provided by the Central Weather Bureau and Water Resources Agency in Taiwan. The MM5 run of Typhoon Zeb was assisted by Mr. Quen-Chi Tung. The MM5 simulations of Typhoon Herb were provided by Profs. Chun-Chieh Wu, Tim-Hau Lee, and Dr. Chia-Huei Chiang at the National Taiwan University. Constructive comments and suggestions of three reviewers improve this paper substantially. The authors are grateful for their support.

REFERENCES

- Blackadar, A. K., 1979: High resolution models of the planetary boundary layer. *Advances in Environmental Sciences and Engineering*, J. Pfafflin and E. Ziegler, Eds., Gordon and Breach, 50–85.
- Chang, S. W.-J., 1982: The orographic effects induced by an island mountain range on propagating tropical cyclones. *Mon. Wea. Rev.*, **110**, 1255–1270.
- Chiang, C.-H., T.-H. Lee, M.-J. Yang, and C.-C. Wu, 2001: Application of a typhoon-based Doppler velocity dealiasing technique (in Chinese). *Proc. 2001 Conf. on Weather Analysis and Forecasting*, Taipei, Taiwan, Central Weather Bureau, 45–50.
- Dudhia, J., 1989: Numerical study of convection observed during the winter monsoon experiment using a mesoscale two-dimensional model. *J. Atmos. Sci.*, **46**, 3077–3107.
- Dutta, D., S. Herath, and K. Musiakke, 2000: Flood inundation simulation in a river basin using a physically based distributed hydrologic model. *Hydrol. Processes*, **14**, 497–519.
- Environmental Systems Research Institute, 1996: ArcView Spatial Analyst Users Manual. 240 pp.
- Faures, J. M., D. C. Goodrich, D. A. Woolhieser, and S. Sorooshian, 1995: Impact of small-scale spatial rainfall variability on runoff modeling. *J. Hydrol.*, **173**, 309–326.
- Ganguly, A. R., and R. L. Bras, 2003: Distributed quantitative precipitation forecasting using information from radar and numerical weather prediction models. *J. Hydrometeorol.*, **4**, 1168–1180.
- Giannoni, F., J. A. Smith, Y. Zhang, and G. Roth, 2003: Hydrologic modeling of extreme floods using radar rainfall estimates. *Adv. Water Resour.*, **26**, 195–203.
- Green, W. H., and G. A. Ampt, 1911: Studies on soil physics. Part I: The flow of air and water through soils. *J. Agric. Sci.*, **4**, 1–24.
- Grell, G., 1993: Prognostic evaluation of assumptions used by cumulus parameterizations. *Mon. Wea. Rev.*, **121**, 764–787.
- , J. Dudhia, and D. R. Stauffer, 1994: A description of the fifth generation Penn State/NCAR Mesoscale Model (MM5). NCAR Tech. Note NCAR/TN-398+STR, 138 pp.
- Ibbitt, R. P., R. D. Henderson, J. Copeland, and D. S. Wratt, 2001: Simulating mountain runoff with meso-scale weather model rainfall estimates: A New Zealand experience. *J. Hydrol.*, **239**, 19–32.
- Jasper, K., J. Gurtz, and H. Lang, 2002: Advanced flood forecasting in Alpine watersheds by coupling meteorological observations and forecasts with a distributed hydrological model. *J. Hydrol.*, **267**, 40–52.
- Lee, W.-C., B. J.-D. Jou, P.-L. Chang, and S.-M. Deng, 1999: Tropical cyclone kinematical structure retrieved from single-Doppler radar observations. Part I: Interpolation of Doppler velocity patterns and the GBVTD technique. *Mon. Wea. Rev.*, **127**, 2419–2439.
- Li, M. H., M. H. Hsu, L. S. Hsieh, and W. H. Teng, 2002: Inundation potential analysis for Tsao-Ling Landslide Lake formed by Chi-chi Earthquake in Taiwan. *Nat. Hazards*, **25**, 289–303.
- Morrison, J. E., and J. A. Smith, 2001: Scaling properties of flood peaks. *Extremes*, **4**, 5–22.
- O'Brien, J. S., P. Y. Julien, and W. T. Fullerton, 1993: Two-dimensional water flood and mudflood simulation. *J. Hydraul. Eng.*, **119**, 244–261.
- , P. Y. Julien, and V. M. Ponce, 1998: FLO-2D users manual for a short course on flooding and mud/debris flow. 61 pp. [Available online at <http://www.flo-2d.com/generic12.html>.]
- Smith, J. A., M. L. Baeck, J. E. Morrison, P. Sturdevant-Rees, D. F. Turner-Gillespie, and P. D. Bates, 2002: The regional hydrology of extreme floods in an urbanizing drainage basin. *J. Hydrometeorol.*, **3**, 267–282.
- Sui, C.-H., and Coauthors, 2002: Meteorology-hydrology study targets typhoon Nari and Taipei flood. *Eos, Trans. Amer. Geophys. Union*, **83**, 265–270.

- Syed, K. H., D. C. Goodrich, D. E. Myers, and S. Sorooshian, 2003: Spatial characteristics of thunderstorm rainfall fields and their relation to runoff. *J. Hydrol.*, **271**, 1–21.
- Thieken, A. H., A. Lücke, B. Diekkrüger, and O. Richter, 1999: Scaling input data by GIS for hydrological modeling. *Hydrol. Processes*, **13**, 611–630.
- Thiessen, A. H., 1911: Precipitation for large areas. *Mon. Wea. Rev.*, **39**, 1082–1084.
- Westrick, K. J., and C. F. Mass, 2001: An evaluation of a high-resolution hydrometeorological modeling system for prediction of a cool-season flood event in a coastal mountainous watershed. *J. Hydrometeorol.*, **2**, 161–180.
- Wigmosta, M. S., L. W. Vail, and D. P. Lettenmaier, 1994: A distributed hydrology-soil-vegetation model for complex terrain. *Water Resour. Res.*, **30**, 1665–1679.
- Wu, C.-C., and Y.-H. Kuo, 1999: Typhoons affecting Taiwan: Current understanding and future challenges. *Bull. Amer. Meteor. Soc.*, **80**, 67–80.
- , T.-H. Yen, Y.-H. Kuo, and W. Wang, 2002: Rainfall simulation associated with Typhoon Herb (1996) near Taiwan. Part I: Topographic effect. *Wea. Forecasting*, **17**, 1001–1015.
- Yang, M.-J., and Q.-C. Tung, 2003: Evaluation of rainfall forecasts over Taiwan by four cumulus parameterization schemes. *J. Meteor. Soc. Japan*, **81**, 1163–1183.
- , and H.-L. Huang, 2004: Precipitation processes associated with the landfalling Typhoon Nari (2001). Preprints, *26th Conf. on Hurricanes and Tropical Meteorology*, Miami, FL, Amer. Meteor. Soc., 134–135.
- Zhang, Y., and J. A. Smith, 2003: Space-time variability of rainfall and extreme flood response in the Menomonee River basin, Wisconsin. *J. Hydrometeorol.*, **4**, 506–517.